Elastic Properties of an Interface of Diblock Copolymer

M. W. Matsen[*,†]

Department of Physics, Simon Fraser University, Burnaby, British Columbia, Canada V5A 1S6

M. Schick[‡]

Sektion Physik der Ludwig-Maximilians-Universität München, 8000 München 2, Germany

Received February 8, 1993; Revised Manuscript Received April 26, 1993

ABSTRACT: A ternary mixture is studied which consists of A and B homopolymers of equal polymerization indices and a symmetric AB diblock copolymer of a smaller index. In addition to A- and B-rich phases, there is a disordered phase in which the A and B homopolymers are solubilized by the copolymer and which coexists with the other two. We calculate, in the weak-segregation limit, the three interfacial tensions and the elastic properties of the A/B interface when there is only a microscopic thickness of copolymer adsorbed there. We find that the saddle-splay modulus is positive, in contrast to results applicable to the strong-segregation limit. The positive ratio of the saddle-splay modulus to the bending modulus is increased if the A and B blocks have different Kuhn lengths. A wetting transition occurs along the triple line.

1. Introduction

In mixtures of incompatible A and B homopolymers, diblock copolymers consisting of blocks of A and B monomers behave much like amphiphiles in mixtures of oil and water.[1] They can cause the two homopolymers to become compatible and bring about a single homogeneous phase, one analogous to the microemulsion in mixtures of oil, water, and amphiphile. This disordered phase is characterized by an extensive amount of internal interface between the homopolymers, an interface which, for the most part, is covered by copolymer. The elastic properties of such internal interfaces are of interest, because from them one can predict the structure within the disordered phase.[2] These elastic properties are defined in terms of a bending free energy per unit area,[3,4]

$$f_{el} = \sigma_0 + \lambda\left(\frac{c_1 + c_2}{2}\right) + 2\kappa\left(\frac{c_1 + c_2}{2}\right)^2 + \bar{\kappa}c_1c_2 \qquad (1)$$

where κ is the bending modulus, $\bar{\kappa}$ is the saddle-splay modulus, c_1 and c_2 are the two local principal curvatures, and $\lambda = -4\kappa c_0$ where c_0 is a preferred or spontaneous curvature.

Several calculations of these moduli have been carried out[5-7] assumming a strong-segregation limit, one with a sharp interface in which the polymers are densely packed and therefore significantly stretched. The most recent of these[7] takes into account the nonuniform density of monomers in the interface by treating it as a grafted polymer brush[8,9] with an adsorption area per copolymer which can adjust to the curvature of the interface. A negative value of $\bar{\kappa}$ is found. As noted by Milner and Witten, this is probably due to the fact that the volume available to the copolymer chains directly above a surface of negative Gaussian curvature, $c_1c_2 < 0$, is reduced with respect to the volume over a flat surface, $c_1 = c_2 = 0$. This reduction in volume must cause a further stretching of chains, and therefore increased energy. Hence a negative value of $\bar{\kappa}$, which disfavors regions of negative Gaussian curvature, is produced. However, a lyotropic phase with negative Gaussian curvature, the ordered bicontinuous double-diamond (OBDD) structure, has been observed in diblock copolymer systems.[10-12] Such a phase would certainly be favored by a positive $\bar{\kappa}$, although it can be thermodynamically stable even for $\kappa < 0$ provided that $-\bar{\kappa}/\kappa$ is not too large.[13]

In this paper, we calculate the elastic properties of a copolymer interface in a manner which differs from that considered above. Whereas previous calculations begin by positing the existence of an interface, we begin with a bulk description of the ternary mixture and, by requiring coexistence, allow the system to produce an interface. We do so because we assume that the internal interfaces in the disordered phase at coexistence are similar to the interface between the A- and B-rich homopolymer phases. Further, we consider the system to be in the weak- rather than strong-segregation limit. The latter case is somewhat simplified because the interface can be considered to be a sharp dividing surface along which the copolymer junctions are confined, and the two phases which it separates can be considered to be pure. In contrast, we consider the continuous distribution of copolymer junctions across the interface and the actual compositions of the homopolymer-rich phases. In principle, our procedure can also be extended to the strong-segregation limit.[14]

Our approach begins with the calculation, *via* the Flory-Huggins theory, of the phase diagram of a ternary mixture containing A and B homopolymers with polymerization index N and AB copolymers of degree N/α, with $\alpha > 1$. This produces a triple line at which A-rich, B-rich, and disordered phases coexist.[15] We then calculate the disorder line in the latter phase[16] within the random-phase approximation[17,18] because we are assured that along the triple line, on the copolymer-rich side of the disorder line, the disordered phase does not wet the A-rich/B-rich homopolymer interface.[19] Thus we will have produced there a microscopically thin layer of copolymer whose elastic properties can be calculated. This is done by expanding the inverse of the structure function, also calculated within the random-phase approximation, to produce the Landau-Ginzburg free energy functional of the system. From this functional, interfacial profiles for a flat interface are obtained, and from these profiles, the interfacial tension and elastic constants can be calculated.[9,20-22] We find that the saddle-splay modulus is positive in this regime. From this result, we would conclude that the disordered phase produced by such a copolymer would be characterized by negative Gaussian

† Present address: Department of Physics FM-15, University of Washington, Seattle, WA 98195.

‡ Permanent address: Department of Physics FM-15, University of Washington, Seattle, WA 98195.

0024-9297/93/2226-3878$04.00/0

curvature and would consist of structures with many handles rather than spherical droplets.

Throughout the calculation, we assume that the A and B blocks have different statistical segment lengths in order to determine the effect of this difference on the calculated quantities. This is motivated by the observation[23] that the OBDD structure is more likely to occur in copolymer systems in which the statistical segment lengths differ appreciably. The effect of this difference on our calculated elastic constants is, in fact, to increase the ratio of $\bar{\kappa}/\kappa$ and thereby to increase the probability of phases with negative Gaussian curvature.

2. The Model

We consider ternary polymer mixtures with volume V, temperature T, and monomer density ρ_0. (We assume monomers are incompressible so that the monomer density is necessarily uniform.) Two of the polymer components are A and B homopolymers, while the third is a diblock AB copolymer. The A homopolymers are each composed of N A monomers, and, similarly, B homopolymers are composed of N B monomers. The copolymers are each composed of $N_{AB} = N/\alpha$ monomers in which the fraction of monomers of type A is $^1/_2$. The fractions of monomers in the system belonging to A homopolymers, B homopolymers, and AB copolymers are given by ϕ_A, ϕ_B, and ϕ_{AB}, respectively. The A and B homopolymers have radii of gyration given by $R_A = (N/6)^{1/2}a_A$ and $R_B = (N/6)^{1/2}a_B$, respectively. The quantities a_A and a_B are the Kuhn statistical lengths of the A and B monomers, respectively. The radius of gyration of the copolymer is then $R_{AB} = [(R_A^2 + R_B^2)/2\alpha]^{1/2}$. We shall take R_{AB} as our length scale in the subsequent calculations. Due to the incompressibility of monomers, the free energy, $\tilde{F}(\eta,\phi)$, depends only on two order parameters which we take to be $\eta \equiv \phi_A - \phi_B$ and $\phi \equiv \phi_{AB}$. In the Flory–Huggins approximation, $\tilde{F}(\eta,\phi)$ is given by

$$\frac{N\tilde{F}(\eta,\phi)}{k_BT\rho_0V} = \frac{1-\phi+\eta}{2}\ln\left(\frac{1-\phi+\eta}{2}\right) + \frac{1-\phi-\eta}{2}\ln\left(\frac{1-\phi-\eta}{2}\right) + \alpha\phi\ln\phi + \frac{N\chi(1-\eta^2)}{4} \quad (1a)$$

Here, χ is the usual Flory–Huggins parameter determining the interaction between unlike monomers in comparison to that between like monomers. For our purposes, it is most convenient to construct the Legendre transform of $\tilde{F}(\eta,\phi)$ with respect to the density ϕ; i.e., $F(\eta,\mu) \equiv \min_\phi[\tilde{F}(\eta,\phi) - \mu\phi V\rho_0]$, where μ is the chemical potential conjugate to the concentration ϕ. The copolymer density is obtained from the chemical potential according to $V\rho_0\mu = \partial\tilde{F}(\eta,\phi)/\partial\phi$ which yields

$$\frac{N\mu}{k_BT} = \alpha - 1 + \alpha\ln\phi - \frac{1}{2}\ln\left(\frac{(1-\phi)^2-\eta^2}{4}\right) \quad (2)$$

It is convenient to express the dependence of $\phi(\eta,\mu)$ on the chemical potential in terms of $\Phi(\mu)$, the copolymer density of the disordered phase with $\eta = 0$. From the above equation, it follows that

$$\frac{N\mu}{k_BT} = \alpha - 1 + \alpha\ln\Phi - \ln\left(\frac{1-\Phi}{2}\right) \quad (3)$$

Using eqs 2 and 3, one obtains $\phi(\eta,\mu)$ from the solution of

$$\left(\frac{1-\phi}{1-\Phi}\right)^2 - \left(\frac{\eta}{1-\Phi}\right)^2 - \left(\frac{\phi}{\Phi}\right)^{2\alpha} = 0 \quad (4)$$

The thermodynamic potential $F(\eta,\mu)$ is now given by

$$\frac{NF(\eta,\mu)}{k_BT\rho_0V} \equiv f(\eta) = \frac{1-\phi+\eta}{2}\ln\left(\frac{1-\phi+\eta}{2}\right) + \frac{1-\phi-\eta}{2}\ln\left(\frac{1-\phi-\eta}{2}\right) + \alpha\phi\ln\phi + \frac{N\chi(1-\eta^2)}{4} - \phi\left[\alpha - 1 + \alpha\ln\Phi - \ln\left(\frac{1-\Phi}{2}\right)\right] \quad (5)$$

The Landau free energy in eq 5 applies to a system with a spatially invariant order parameter η. To account for slow spatial variations in this order parameter, we generalize this free energy to the following Landau–Ginzburg free-energy functional,

$$\frac{NF[\eta(\vec{r}),\mu]}{k_BT\rho_0} = \int\{h(\eta)[R_{AB}^2\nabla^2\eta]^2 + g(\eta)[R_{AB}\nabla\eta]^2 + f(\eta)\}\,d^3r \quad (6)$$

We have included a Laplacian squared term as well as a gradient squared term, because the situation will arise in which $g(\eta)$ becomes negative. We consider only positive values for $h(\eta)$ by restricting the values of α considered. In particular, α must not become too large. The functions $g(\eta)$ and $h(\eta)$ are obtained from the η–η structure function by expanding its inverse in powers of q^2,[22]

$$\frac{N}{2\rho_0}S_{\eta\eta}^{-1}(q) = \frac{1}{2}f''(\eta) + g(\eta)[qR_{AB}]^2 + h(\eta)[qR_{AB}]^4 + O([qR_{AB}]^6) \quad (7)$$

In the random-phase approximation, the η–η structure function is given by[24]

$$\rho_0^2S_{\eta\eta}(q) = \frac{4S_AS_B + (S_A+S_B)S_C - 2\chi\rho_0^{-1}(S_AS_BS_D + (S_A+S_B)D)}{S_A+S_B+S_C-2\chi\rho_0^{-1}(S_AS_B+S_AS_{BB}+S_BS_{AA}+D)} \quad (8)$$

where

$$S_C = S_{AA} + S_{BB} + 2S_{AB} \quad (9)$$

$$S_D = S_{AA} + S_{BB} - 2S_{AB} \quad (10)$$

$$D = S_{AA}S_{BB} - S_{AB}^2 \quad (11)$$

Here S_A and S_B denote the monomer-concentration correlation functions of independent A- and B-homopolymer chains, respectively. Treating them as ideal Gaussian chains, one obtains

$$S_A(q) = \rho_0\phi_ANd(1,(qR_A)^2) \quad (12)$$

$$S_B(q) = \rho_0\phi_BNd(1,(qR_B)^2) \quad (13)$$

where the function

$$d(r,x) = 2(rx + e^{-rx} - 1)x^{-2} \quad (14)$$

is the Debye scattering function. The S_{AA}, S_{BB}, and S_{AB} are A–A, B–B, and A–B monomer correlation functions of independent diblock copolymer chains. In the same ideal limit,

$$S_{AA}(q) = \frac{\rho_0\phi_{AB}N}{\alpha}d\left(\frac{1}{2},\frac{(qR_A)^2}{\alpha}\right) \quad (15)$$

$$S_{BB}(q) = \frac{\rho_0\phi_{AB}N}{\alpha}d\left(\frac{1}{2},\frac{(qR_B)^2}{\alpha}\right) \quad (16)$$

$$S_{AB}(q) = \frac{\rho_0\phi_{AB}N}{\alpha}\left[\frac{(qR_A)^2}{2\alpha}d\left(\frac{1}{2},\frac{(qR_A)^2}{\alpha}\right) - \frac{1}{2}\right] \times \left[\frac{(qR_B)^2}{2\alpha}d\left(\frac{1}{2},\frac{(qR_B)^2}{\alpha}\right) - \frac{1}{2}\right] \quad (17)$$

Expansion of the expression for the η–η structure function (eq 8) gives

$$g(\eta) = \left[\frac{\Upsilon_1\alpha}{6\psi^2} - \frac{\phi(N\chi)^2}{48\alpha}\right] + \left[\frac{\Upsilon_2\alpha}{6\psi^2} - \frac{\phi N\chi}{24\psi}\right]\eta\gamma \quad (18)$$

$$h(\eta) = \left[\frac{\Upsilon_3\alpha}{72\psi^3} + \frac{\phi(N\chi)^2}{128\alpha} - \frac{\phi^2(N\chi)^3}{576\alpha^2}\right] + \left[\frac{\Upsilon_4\alpha}{288\psi^3} + \frac{\Upsilon_5\phi N\chi}{576\psi^2} + \frac{\phi^2(1-\phi)(N\chi)^2}{1152\alpha\psi}\right]\gamma^2 + \left[\frac{\Upsilon_6\alpha^2}{36\psi^3} + \frac{\Upsilon_7\phi N\chi}{288\psi^2} - \frac{\phi^2(N\chi)^2}{288\alpha\psi}\right]\eta\gamma \quad (19)$$

where

$$\gamma = \frac{a_A^2 - a_B^2}{a_A^2 + a_B^2} \quad (20)$$

is a measure of the difference in Kuhn lengths. The various coefficients are

$$\Upsilon_1 = (1-\phi)(\alpha+\phi-\alpha\phi)^2 + [\phi - 2\alpha\phi - \alpha^2(1-\phi)]\eta^2$$

$$\Upsilon_2 = \phi^2 - \alpha^2(1-\phi)^2 + \alpha^2\eta^2$$

$$\Upsilon_3 = \alpha(1-\phi)^2(\alpha+\phi-\alpha\phi)^3 + [\phi^2(1-\phi) - 3\alpha\phi(1-\phi)^2 + \alpha^2\phi(8-19\phi+11\phi^2) - 9\alpha^3\phi(1-\phi)^2 - 2\alpha^4(1-\phi)^3]\eta^2 + [3\alpha\phi - 8\alpha^2\phi + 6\alpha^3\phi + \alpha^4(1-\phi)]\eta^4$$

$$\Upsilon_4 = 4\alpha(1-\phi)^2(\alpha-3\phi-\alpha\phi)(\alpha+\phi-\alpha\phi)^2 - [3\phi^2(1-\phi) + \alpha\phi(3-6\phi-13\phi^2) - 20\alpha^2\phi^2(1-\phi) + 4\alpha^3\phi(1-\phi)^2 + 8\alpha^4(1-\phi)^3]\eta^2 + [3\alpha\phi + 8\alpha^3\phi + 4\alpha^4(1-\phi)]\eta^4$$

$$\Upsilon_5 = 8\alpha(1-\phi)^2(\alpha+\phi-\alpha\phi) - [\phi + 8\alpha\phi + 8\alpha^2(1-\phi)]\eta^2$$

$$\Upsilon_6 = -\phi^2(4-9\phi+5\phi^2) - \alpha\phi(4-9\phi)(1-\phi)^2 + 3\alpha^2\phi(1-\phi)^3 - \alpha^3(1-\phi)^4 + [4\phi^2 + \alpha\phi(4-9\phi) - 3\alpha^2\phi(1-\phi) + 2\alpha^3(1-\phi)^2]\eta^2 - \alpha^3\eta^4$$

$$\Upsilon_7 = (3-4\alpha)\psi - 4(1-\alpha)\phi(1-\phi)$$

$$\psi = (1-\phi)(\alpha+\phi-\alpha\phi) - \alpha\eta^2$$

Note that the order parameter η and the measure of the difference in Kuhn lengths γ are both odd under the interchange of the *labels* A and B. It is easy to see from the above that the Landau–Ginzburg functional is invariant under this interchange, as it must be.

3. Phase Diagram

We first consider the critical line separating the disordered phase from the coexisting A- and B-rich phases. By expanding the free energy per monomer $f(\eta)$ of eq 5, in powers of η, we obtain

$$f(\eta) = f(0) + \frac{1}{2}\left[\frac{1}{1-\Phi} - \frac{N\chi}{2}\right]\eta^2 + \frac{2\alpha - \Phi - 2\alpha\Phi}{24(1-\Phi)^3(\alpha+\Phi-\alpha\Phi)}\eta^4 + O(\eta^6) \quad (21)$$

The critical line at which the disordered phase undergoes a continuous transition to A- and B-rich phases occurs for $\eta = 0$ when $f''(0) = 0$, which gives the relation between critical values of χ and concentration ϕ to be $N\chi_c = 2/(1-\phi)$ with $\phi = \Phi$. As ϕ increases from 0, $N\chi_c$ increases from 2. If $\alpha < 1$, this critical line terminates at a Lifshitz critical point at which $g(0)$ vanishes.[15] From eq 18, this coefficient is given by

$$g(0) = \frac{1}{6}\left[\frac{\alpha}{1-\Phi} - \frac{\Phi(N\chi)^2}{8\alpha}\right] \quad (22)$$

which vanishes when $N\chi_c = 2 + 4\alpha^2$. Beyond the Lifshitz point, the disordered phase undergoes a transition to a lamellar phase. When $\alpha > 1$, the critical line terminates at a tricritical point at which $f''(0) = f''''(0) = 0$. From eq 21, this occurs when $N\chi_c = 2 + 4\alpha$.[15] Beyond the tricritical point is a line of three-phase coexistence between A-rich, B-rich, and disordered phases. This line terminates at a four-phase point at which the lamellar phase coexists with the other three phases. Beyond this point, the disordered phase makes a transition directly to the lamellar phase. When $\alpha = 1$, the Lifshitz and tricritical points coincide, producing a Lifshitz tricritical point.[15,16] We consider the case where the critical line terminates at a tricritical point in order to study the disordered phase at coexistence with the A and B homopolymer-rich phases.

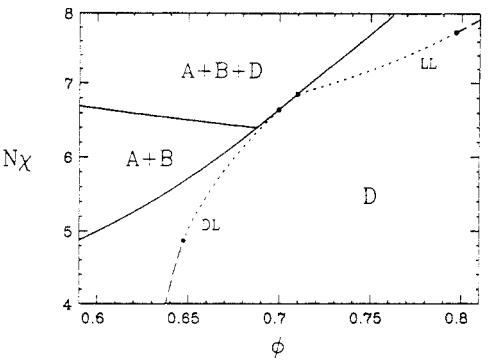

Figure 1. Phase diagram in the vicinity of the tricritical point for $\alpha = 1.1$. The symbols A, B, and D denote the A-rich, B-rich, and disordered phases. The disorder line (DL) and Lifshitz line (LL) in the disordered phase are drawn with dashed lines.

The determination of the triple line of this model is simplified because the Landau free energy (eq 5) is an even function of the order parameter η. The triple line occurs when χ and Φ are such that $f(\eta_A) = f(0)$ and $f'(\eta_A) = 0$ for some positive η_A. This is the value of the order parameter in the A-rich phase, and, by symmetry, the value in the B-rich phase is $-\eta_A$. The copolymer density of the disordered phase is Φ, and in the A- and B-rich phases it is $\phi(\eta_A)$, obtained by solving eq 4. For the case $\alpha = 1.1$, the phase diagram in the vicinity of the tricritical point is shown in Figure 1. The four-phase point occurs at $N\chi \approx 8$, and the lamellar phase for larger $N\chi$. The figure does not encompass this region.

In addition to the phase boundaries, Figure 1 shows the disorder and Lifshitz lines in the disordered phase. The significance of these lines is that they indicate where the disordered phase exhibits microemulsion structure. The disorder line is the locus of points at which the asymptotic behavior of a general correlation function changes from a monotonic exponential decay, exhibited on the low copolymer concentration side of the line, to an exponentially damped oscillatory decay, on the high concentration side. The latter behavior reflects the tendency of the copolymer to order the homopolymers and thus can be taken as an indicator of microemulsion behavior. The Lifshitz line is a marker of a more developed microemulsion structure. It is the locus of points at which the oscillations

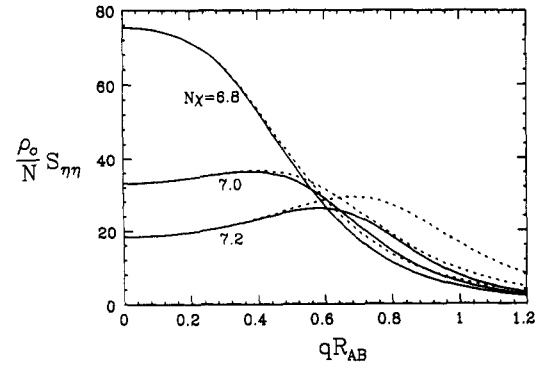

Figure 2. η–η structure function shown along the triple line for several values of $N\chi$. The solid lines are obtained using the expression in eq 8, and the dashed lines are from the truncated series in eq 7.

in the correlation function are sufficient to produce the dominant peak in the associated structure function at nonzero wavevector. The peak is at nonzero wavevector on the high copolymer concentration side of the Lifshitz line. Whereas the disorder line is a property of all correlation functions in general, a Lifshitz line is associated with a specific structure function; i.e., the tendency to order dominates different correlation functions at different concentrations of copolymer. We calculate the Lifshitz line for the η–η structure function.

The asymptotic behavior of a correlation function is governed by the pole in the related structure function with the smallest imaginary part. If the relevant pole is purely imaginary, then the correlation function decays monotonically at large distances, but if it is complex, the function exhibits oscillations as it decays. (Note that a pole at real q implies the disordered phase is unstable.) The change in asymptotic behavior can occur in two ways:[25] a double imaginary pole can split into complex-conjugate poles or the imaginary part of a pair of complex poles can become smaller than that of a purely imaginary one. The former case occurs as the portion of the calculated disorder line shown as a short-dash line in Figure 1 is crossed; on traversing the long-dash segment of the disorder line shown schematically beyond the dot, the latter case occurs.

On the Lifshitz line in Figure 1, $g(0) = 0$ and $h(0) > 0$. In this case, the peak in $S_{\eta\eta}(q)$ at $q = 0$ moves continuously to nonzero q as the line is crossed. Figure 2 illustrates this progression along the triple line, for which case the Lifshitz line occurs at $N\chi = 6.8543$. The dot at the right end of the calculated Lifshitz line in Figure 1 marks the point at which $h(0) = 0$. Beyond this, a peak grows at $q \neq 0$, while the peak at $q = 0$ remains. One can extend to the right of this point an equimaxima line, which indicates where the two peaks are equal in magnitude.[16] A small portion of this line is shown schematically in Figure 1. Figure 2 also shows that the approximation of $S_{\eta\eta}^{-1}$ by the first three terms in a power series (eq 7) becomes less adequate as one goes to increasingly larger values of χ along the triple line (*i.e.*, the strong-segregation limit).

The disorder and Lifshitz lines in Figure 1 are calculated for equal statistical segment lengths, $\gamma = 0$. Although the Lifshitz line does not change with γ, the point at which $h(0) = 0$ moves toward the triple line as the magnitude of γ increases. With $\alpha = 1.1$, the portion of the Lifshitz line with $h(\eta) > 0$ remains for all γ, but this is not the case when α gets much larger. The position of the disorder line is rather insensitive to the value of γ. The main effect of such a change is that the portion of the line shown in Figure 1, at which a pair of imaginary poles become a complex-conjugate pair, becomes shorter. For $\alpha = 1.1$, the portion of the line shown does not go to zero even for the maximum value $\gamma = \pm 1$ but does so for larger α.

4. A/B Interface along the Triple Line

We consider a flat A-rich/B-rich interface perpendicular to the z-direction so that η is a function only of the dimensionless coordinate $\zeta = z/R_{AB}$. Minimization of the Landau–Ginzburg free-energy functional in eq 6 produces a fourth-order Euler–Lagrange equation with the first integral[19]

$$2h'(\eta)\,[\eta']^2\eta'' + h(\eta)\,[2\eta'\eta''' - (\eta'')^2] - g(\eta)\,[\eta']^2 + f(\eta) = f(\eta_A) \quad (23)$$

where $f(\eta_A)$ is the value of the free energy density in any of the three coexisting bulk phases. The boundary conditions on the profile are that $\eta(-\infty)$ is equal to the value of η in the bulk phase on one side of the interface and that $\eta(\infty)$ equals the value of η in the bulk phase on the other. To make the spontaneous curvature and saddle-splay modulus unique, we impose the condition that $\zeta = 0$ corresponds to the equimolar surface[20]

$$\int_{-\infty}^{0}[\eta(\zeta) - \eta_A]\,d\zeta + \int_{0}^{\infty}[\eta(\zeta) + \eta_A]\,d\zeta = 0 \quad (24)$$

The solution of eq 23 is not unique; there are a countable number from which we select the one with the lowest interfacial tension given by eq 25 below.

Once $\eta(\zeta)$ is known, one can calculate[20,21] the surface tension σ, the spontaneous-curvature modulus λ, the bending rigidity κ, and the saddle-splay modulus $\bar{\kappa}$ using

$$\frac{N\sigma}{k_B T \rho_0 R_{AB}} = \int_{-\infty}^{+\infty} p_s\,d\zeta \quad (25)$$

$$\frac{N\lambda}{k_B T \rho_0 R_{AB}^2} = 2\int_{-\infty}^{+\infty} \zeta p_s\,d\zeta \quad (26)$$

$$\frac{N\kappa}{k_B T \rho_0 R_{AB}^3} = 2\int_{-\infty}^{+\infty} h(\eta)[\eta']^2\,d\zeta \quad (27)$$

$$\frac{N(\bar{\kappa} - 2\kappa)}{k_B T \rho_0 R_{AB}^3} = \int_{-\infty}^{+\infty} \zeta^2 p_s\,d\zeta \quad (28)$$

where

$$p_s \equiv 2g(\eta)\,[\eta']^2 + 4h(\eta)\,[\eta'']^2 \quad (29)$$

With our boundary conditions, a positive value of λ corresponds to a spontaneous curvature toward the B homopolymers which, for $\gamma > 0$, are the ones with shorter statistical segment length. Equations 25–29 are derived by using the Landau free energy of eq 5 to calculate the free energy per unit area of a cylindrical and of a spherical interface in a power series in the curvatures of these geometries. On comparing the result, term by term, to the bending free energy of eq 1, the above expressions for the coefficients σ, λ, κ, and $\bar{\kappa}$ follow. The function $p_s(\zeta)$ is interpreted as the stress profile across the interface.

After the calculation of all three interfacial tensions along the triple line, the question of whether the A/B interface is wetted by the disordered phase can be addressed. We find, as expected, that on the low-temperature (large-χ) side of the disorder line the interface is not wetted, $\sigma_{AB} < \sigma_{AD} + \sigma_{BD}$, while above it, it is, $\sigma_{AB} = \sigma_{AD} + \sigma_{BD}$. The wetting transition occurs when $g^2(0) - 2h(0)\,f''(0) = 0$, which is the location of the disorder line obtained from the approximation to the structure function in eq 7. Were it not for this expansion, we believe that the transition would occur exactly at the disorder line.[19]

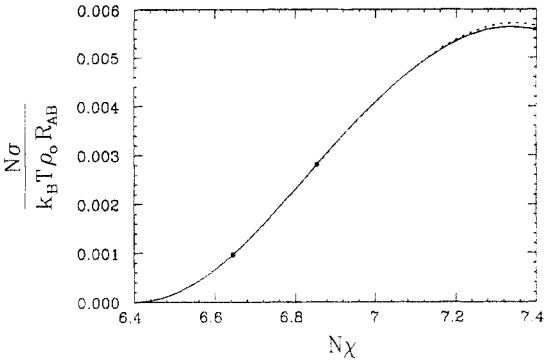

Figure 3. A/B interfacial tension along the A + B + D triple line at $\alpha = 1.1$. The solid and dashed lines correspond to $\gamma = 0$ and $\gamma = \pm 1$, respectively. The dots show the locations of the disorder and Lifshitz lines. The disorder line does shift as γ is varied, but not sufficiently to be noticed on the scale of this plot.

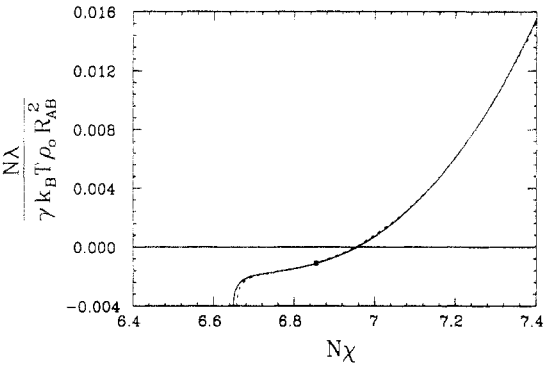

Figure 4. Spontaneous-curvature modulus of the A/B interface along the triple line. The solid and dashed lines correspond to $\gamma \to 0$ and $\gamma = \pm 1$, respectively. The dot shows the location of the Lifshitz point.

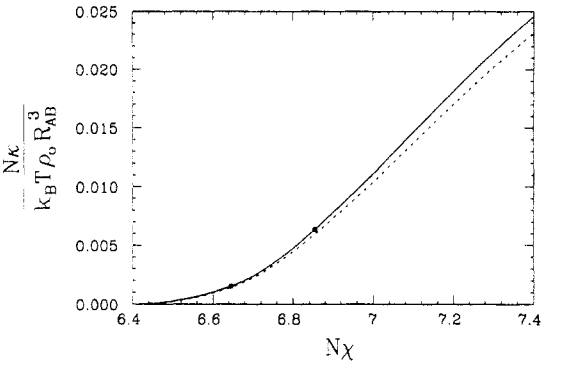

Figure 5. Bending rigidity of the A/B interface along the triple line. The solid and dashed lines correspond to $\gamma = 0$ and $\gamma = \pm 1$, respectively. The dots show the locations of the disorder and Lifshitz lines.

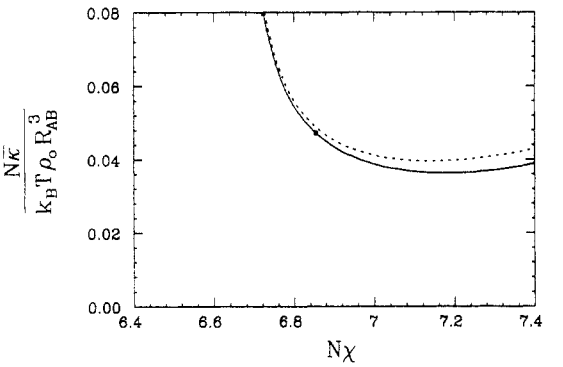

Figure 6. Saddle-splay modulus of the A/B interface along the triple line. The solid and dashed lines correspond to $\gamma = 0$ and $\gamma = \pm 1$, respectively. The dot shows the location of the Lifshitz line.

At values of χ larger than χ_w at which the wetting transition occurs, an equilibrium width, l, of the disordered phase exists between the A- and B-rich bulk phases. As the wetting transition, χ_w, is approached from above, this width diverges as $l \sim (\chi - \chi_w)^{-1/2}$.[19] Hence, the transition is continuous. We also note that, just above the wetting transition, $\lambda \approx -l(\sigma_{AD} - \sigma_{BD})$ and $\bar{\kappa} \approx l^2\sigma_{AB}/4$. Consequently, both quantities diverge as $\chi \to \chi_w^+$ and are undefined when the interface is wet.

We suspect that the wetting transition is second order when the pole with the smallest imaginary part changes from purely imaginary to complex and that it is first order when the imaginary part of a complex pole simply becomes smaller than that of a purely imaginary one. A tricritical wetting transition would separate these two regions. Our approximations are too restrictive to investigate this possible change to a first-order wetting transition, which should occur as α is increased. First, $h(\eta)$ tends to become negative as α increases which would make the free energy of eq 6 unbounded from below. Second, we would have to keep terms up to sixth order in the expansion of eq 7 to describe this scenario. In any event, the inclusion of long-range van der Waals forces is expected to drive the wetting transition to be first order and to cause it to occur on the microemulsion side of the disorder line[19] as is observed in ternary oil–water–amphiphile systems.[26]

Figures 3–6 show the surface tension σ, spontaneous-curvature modulus λ, bending rigidity κ, and saddle-splay modulus $\bar{\kappa}$, respectively, of the A/B interface along the triple line. The solid lines correspond to $\gamma = 0$, and the dashed lines, to the limiting values $\gamma = \pm 1$. These plots show that σ is almost independent of γ. It vanishes at the tricritical point and reaches a maximum along the triple line. We expect that the interfacial tension would be ultralow in the vicinity of the four-phase point as it is in ternary oil–water–amphiphile systems,[19,27] but we cannot extend this calculation to this point as we noted earlier. The curvature modulus λ is essentially linear in γ, as might be anticipated. This is readily seen by noting that the quantity λ/γ, which is plotted in Figure 4, is nearly independent of γ. The moduli κ and $\bar{\kappa}$ depend weakly on γ, but the effects can be on the order of 10%. Furthermore, κ decreases with $|\gamma|$ while $\bar{\kappa}$ increases, so that there can be an effect of order 20% in their ratio. The increase in this ratio would tend to favor phases with a negative Gaussian curvature. In each figure, the intersection of the Lifshitz line with the triple line is marked with a dot at $N\chi = 6.8543$. The plots of σ and $\bar{\kappa}$, quantities defined on both sides of the wetting transition, have a dot marking the location of the disorder line as well.

Figures 7 and 8 show the order parameter, η, and the stress, p_s, for a wide and narrow interface, respectively. The solid lines correspond to $\gamma = 0$ and the dashed lines to $\gamma = 1$. One can see that an increase of the Kuhn length of A with respect to that of B which causes $\gamma > 0$ increases the stress on the B-rich side, $\zeta > 0$, of the narrow interface and decreases it on the A-rich side. The opposite occurs near the wetting transition where the interface is thick. The result is that the thin interface spontaneously curves toward the B-rich phase which has the smaller Kuhn length, as might be expected intuitively. The thick interface does the opposite. In both cases, the curvature acts to reduce the volume where the stress is large in order to lower the interfacial energy.

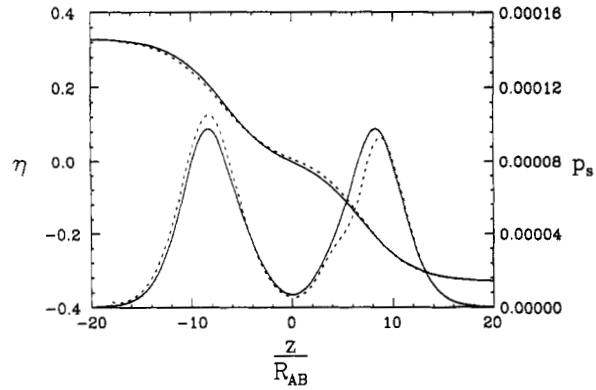

Figure 7. Order parameter, η, and stress, p_s, across the A/B interface at $N\chi = 6.7$ on the triple line. The solid and dashed lines correspond to $\gamma = 0$ and 1, respectively.

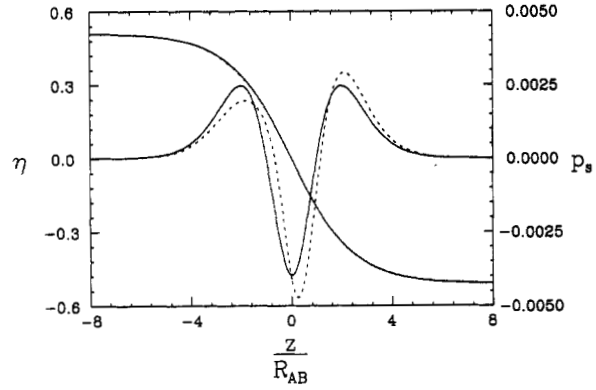

Figure 8. Same as Figure 7 except for $N\chi = 7.2$.

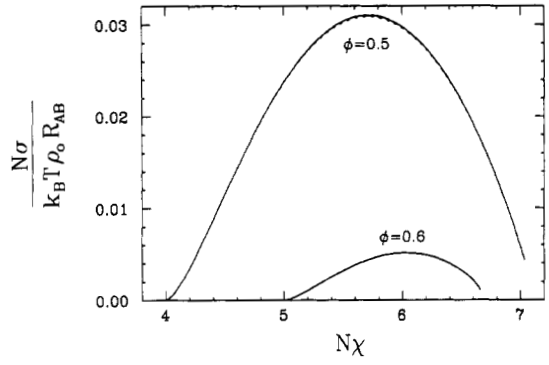

Figure 9. A/B interfacial tension along two paths of constant copolymer density in the A + B region for $\alpha = 1.1$. Each path extends from the consolute line up to the triple line. The solid and dashed lines correspond to $\gamma = 0$ and $\gamma = \pm 1$, respectively.

5. A/B Interface in the A + B Region

For completeness, we examine the A/B interface in the A + B coexistence region. We concentrate on two paths through this region with constant copolymer concentrations and $\alpha = 1.1$. We select paths with $\phi = 0.5$ and 0.6. These paths extend from the second-order line at $N\chi = 4.0$ and 5.0 to the triple line at $N\chi = 7.0339$ and 6.6607, respectively.

Figures 9–12 show the surface tension σ, spontaneous-curvature modulus λ, bending rigidity κ, and saddle-splay modulus $\bar{\kappa}$ along these two paths of constant bulk copolymer density. Again, σ is weakly dependent on γ, and λ depends nearly linearly on it. These figures illustrate that the addition of copolymer at constant χ tends to reduce each quantity. They also show that each quantity vanishes at the second-order line, increases with increasing χ until a peak is reached, and then decreases as the triple line is approached. When the triple line is approached at a point

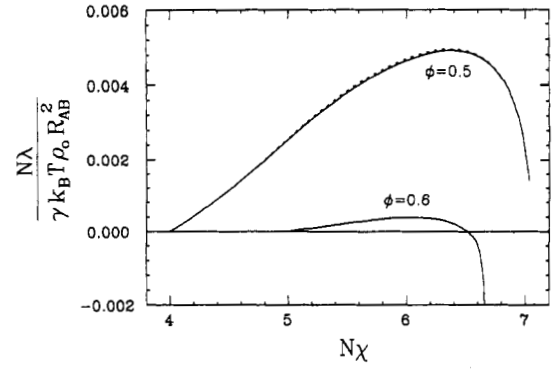

Figure 10. Spontaneous-curvature modulus of the A/B interface along two paths of constant copolymer density in the A + B region. The solid and dashed lines correspond to $\gamma \to 0$ and $\gamma = \pm 1$, respectively.

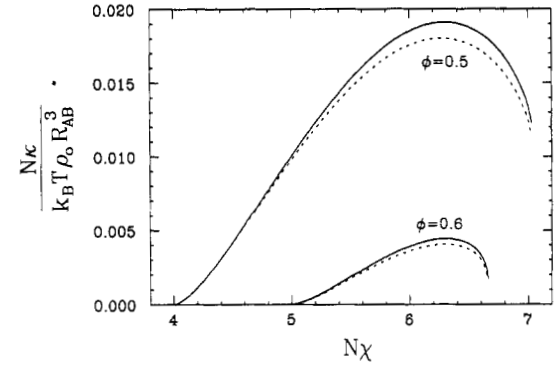

Figure 11. Bending rigidity of the A/B interface along two paths of constant copolymer density in the A + B region. The solid and dashed lines correspond to $\gamma = 0$ and $\gamma = \pm 1$, respectively.

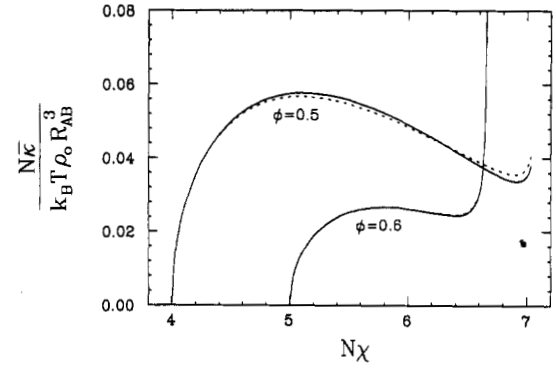

Figure 12. Saddle-splay modulus of the A/B interface along two paths of constant copolymer density in the A + B region. The solid and dashed lines correspond to $\gamma = 0$ and $\gamma = \pm 1$, respectively.

at which the disordered phase wets the A/B interface, λ/γ and $\bar{\kappa}$ diverge to minus and plus infinity, respectively. The path shown for $\phi = 0.6$ intercepts the triple line near the wetting transition, but to the nonwet side of it. Hence, neither λ nor $\bar{\kappa}$ diverge, although they do become quite large in magnitude. Generally, λ/γ is a positive quantity so that the A/B interface spontaneously curves toward the phase rich in the shorter homopolymer. However, when approaching a three-phase coexistence occurring at a value of $N\chi$ less than about seven, λ/γ becomes negative.

6. Conclusion

We have employed the random-phase approximation to generate a Landau–Ginzburg free-energy functional which describes the weak-segregation limit of a ternary, polymer system consisting of A and B homopolymers and AB copolymers. With the polymerization index of the

copolymer chosen to be less than that of the homopolymers, coexistence occurs between the A-rich, B-rich, and disordered phases. In the latter phase, the homopolymers are solubilized by the copolymer. Beyond the disorder line, the interface between A- and B-rich phases is not wetted by the disordered phase, so that only a microscopically thin layer of copolymer exists there. It was assumed that this interface is very much like the internal interfaces within the disordered system; *i.e.*, the disordered phase, on the high copolymer concentration side of the disorder line, is viewed as being comprised of coherent regions of A monomers separated from coherent regions of B monomers by well-defined internal interfaces which comprise a small fraction of the volume. Interfacial profiles were calculated, and, from them, the three interfacial tensions were obtained, as were the elastic properties of the A/B interface. We found that the saddle-splay modulus was positive in contrast to calculations in the strong-segregation limit in which it is found to be negative. From this we infer that the disordered phase would be characterized by interfaces with negative Gaussian curvature. We found that this tendency was enhanced when the A and B monomers had different Kuhn lengths. Finally we showed that a wetting transition would occur along the line of three-phase coexistence. Such transitions have been observed in the analogous ternary water–oil–amphiphile systems.[28] Recent experiments on wetting in polymer systems[29] encourage us to believe that these transitions should also be observable.

Acknowledgment. M.S. thanks Frank Bates for a stimulating and thoroughly enjoyable series of conversations. He also is grateful to the Alexander von Humboldt-Stiftung for a Senior Scientist Award and to Prof. Herbert Wagner for his hospitality at the Ludwig-Maximilians Universität. M.W.M. thanks Michael Plischke and Michael Wortis for their hospitality at Simon Fraser University. This work was supported in part by the National Science Foundation under Grant No. 8916052 and by the Natural Sciences and Engineering Research Council of Canada.

References and Notes

(1) Maglio, G.; Palumbo, R. *Polymer Blends*; Kryszewski, M., Galeski, A., Martuscelli, E., Eds.; Plenum: New York, 1982.
(2) Safran, S. A.; Turkevich, L. A.; Pincus, P. A. *J. Phys. (Paris) Lett.* **1984**, *45*, L-19.
(3) Helfrich, W. *Z. Naturforsch. C* **1973**, *28*, 693.
(4) Canham, P. B. *J. Theor. Biol.* **1970**, *26*, 61.
(5) Cantor, R. S. *Macromolecules* **1981**, *14*, 1186.
(6) Leibler, L. *Makromol. Chem., Macromol. Symp.* **1988**, *16*, 1.
(7) Wang, Z.-G.; Safran, S. A. *J. Chem. Phys.* **1991**, *94*, 679.
(8) Semenov, A. N.; *Sov. Phys. JETP* **1985**, *61*, 733.
(9) Milner, S. T.; Witten, T. A. *J. Phys. (Paris)* **1988**, *49*, 1951.
(10) Thomas, E. L.; Alward, D. B.; Kinning, D. J.; Martin, D. C.; Handlin, D. L.; Fetters, L. J. *Macromolecules* **1986**, *19*, 2197.
(11) Hasegawa, H.; Tanaka, H.; Yamasaki, K.; Hashimoto, T. *Macromolecules* **1987**, *20*, 1651.
(12) Bates, F. S. *Science* **1991**, *251*, 898.
(13) Wang, Z.-G.; Safran, S. A. *Europhys. Lett.* **1990**, *11*, 425.
(14) Ohta, T.; Kawasaki, K. *Macromolecules* **1986**, *19*, 2621. Anderson, D. M.; Thomas, E. L. *Macromolecules* **1988**, *21*, 3221.
(15) Broseta, D.; Fredrickson, G. H. *J. Chem. Phys.* **1990**, *93*, 2927.
(16) Holyst, R.; Schick, M. *J. Chem. Phys.* **1992**, *96*, 7728.
(17) de Gennes, P.-G. *J. Phys. (Paris)* **1970**, *31*, 235.
(18) Leibler, L. *Macromolecules* **1980**, *13*, 1602.
(19) Gompper, G.; Schick, M. *Phys. Rev. Lett.* **1990**, *65*, 1116.
(20) Gompper, G.; Zschocke, Z. *Europhys. Lett.* **1991**, *16*, 731.
(21) Gompper, G.; Zschocke, Z. *Phys. Rev.* **1992**, *A46*, 4836.
(22) Lerczak, J.; Schick, M.; Gompper, G. *Phys. Rev. A* **1992**, *46*, 985.
(23) Bates, F. S.; Schultz, M. F.; Rosedale, J. H. *Macromolecules* **1992**, *25*, 5547.
(24) Leibler, L. *Macromolecules* **1982**, *15*, 1283.
(25) Matsen, M. W.; Sullivan, D. E. *Phys. Rev. A* **1992**, *46*, 1985.
(26) Schubert, K.-V.; Strey, R. *J. Chem. Phys.* **1991**, *95*, 8532.
(27) Aratono, M.; Kahlweit, M. *J. Chem. Phys.* **1991**, *95*, 8578.
(28) Kahlweit, M.; Strey, R.; Aratono, M.; Busse, G.; Jen, J.; Schubert, K.-V. *J. Chem. Phys.* **1991**, *95*, 2842.
(29) Steiner, U.; Klein, J.; Eisner, E.; Budkowski, A.; Fetters, L. *Science* **1992**, *258*, 1126.